Chapter 4

Spatial Scaling of Dorsal-Ventral Patterns in the Early *Drosophila* Embryo

Animal populations naturally display variations in the size of their individuals, but these changes in total size are often compensated by proportional changes in organ or tissue sizes. This phenomenon, commonly referred to as scaling, is widespread in animals, but the mechanisms by which cells acquire *relative* positional coordinates -- so that patterns correlate with the size of the field -- are poorly understood. Patterning of the dorsal-ventral (DV) axis in the early *Drosophila* embryo depends on the nuclear distribution of the maternal factor Dorsal (dl). Using quantitative fluorescent *in situ* hybridization data, we investigate how the location of dl target genes depends on natural variations in the size of the DV axis. We show that the borders of the dl target genes *vnd* and *sog* scale with the size of the system, while the *ind* borders correlate, but do not strictly scale with the length of the DV axis. Our results suggest that scaling in this system is a gene-dependent rather than a position-dependent property. The width of the nuclear dl gradient also correlates with axis length, but is not sufficient to explain strict scaling of DV patterns directly in a concentration-dependent manner. Using a system in which a gradient of nuclear dl is ectopically generated along the anterior-posterior (AP) axis, we asked whether scaling solely depends on the patterning cascade downstream of dl or if other endogenous factors contribute to spatial scaling along the DV axis. We found that dl nuclear gradient exhibits much variability and does not scale with respect to the AP axis in these embryos. Strikingly, however, the posterior border of the *vnd* pattern scales precisely with the length of the AP axis. Since the ectopic dl gradient is the only source

of DV positional information in these embryos, we conclude that factors downstream of dl provide spatial information relative to the length of the axis.

4.1 Introduction

Scaling, the ability of pattern to correlate with size in an embryonic field, is exhibited at different levels of organization in animal development. At the level of a single organism, animals often display the ability to reorganize their patterning programs after surgical manipulations; for example, amphibian embryos that are cut in half or fused to other embryos maintain the proportions of their patterns and give rise to anatomically normal animals of different sizes (Spemann, 1938). Another aspect of scaling at the single animal level is the ability of patterns to accommodate changes in size as a result of tissue growth. Many developing systems that are genetically or environmentally manipulated to over- or under-grow are able to maintain the proportions of their patterns invariant. For instance, fly larvae that are poorly fed produce flies with smaller wings, but the wing venation pattern remains largely unaffected (Robertson, 1963).

A different aspect of scaling phenomena is exhibited at the species level; groups of closely related species that differ substantially in egg size give rise to anatomically similar animals despite the fact that they use much of the same genetic circuitry (Carroll et al., 2005). A particular case of this form of scaling is the ability of a population of embryos from a single species to maintain pattern proportions despite natural variations in the size of their individuals. However, there is a fundamental difference between scaling across species and scaling within a species; while scaling across species can be afforded by the adaptation of patterning molecules to evolutionary changes in size,

scaling within a homogeneous population of organisms must rely on a mechanism of establishing positional information using a system of relative, rather than absolute coordinates. Although this form of scaling is widespread in the animal kingdom, the detailed mechanisms by which cells acquire positional information relative to size remain largely unknown.

The *Drosophila* embryo has become a useful system to study spatial scaling of patterns in response to natural variations in embryo size as it provides the following advantages. First, the size of an embryo remains practically unchanged once it is laid and, therefore, a single measurement of axis length is enough to describe the "size" of the system over the whole patterning process. Second, gene expression patterns can be measured quantitatively with resolution that is not yet possible in other systems. Recent studies have compared scaling of Bicoid (Bcd)-dependent patterns along the AP axis in *Drosophila* embryos with scaling of the Bcd gradient itself. For example, a study on closely related *Drosophila* species shows that segmentation patterns in the embryo scale along the AP axis despite that the diffusion properties of Bcd were predicted to be the same in different species (Gregor et al., 2005; Gregor et al., 2008). Further studies have demonstrated that gap gene patterns scale despite natural variations of egg length, even within the same species (Gregor et al., 2007; He et al., 2008; Holloway et al., 2006; Lott et al., 2007; de Lachapelle and Bergmann, 2010), suggesting that the property of scaling in this system is likely to depend on a mechanism of "sensing" the size of the embryo, rather than on the evolution of the biochemical properties of the Bcd morphogen. These studies have established the *Drosophila* embryo as a model system to study scaling of pattern in response to natural variations in size.

Although scaling along the AP axis of the *Drosophila* embryo has been recently the focus of much attention, little is known about scaling along the dorsal-ventral (DV) axis. DV patterning in the fly embryo is orchestrated by the maternal factor Dorsal (dl), a NF-κB homolog (reviewed by Moussian and Roth, 2005). Maternal dl is ubiquitously present in the embryo cytoplasm where it is sequestered by the IκB homolog, Cactus. However, upon activation of the Toll transmembrane receptor in the ventral side of the embryo by the Spätzle morphogen, Cactus is targeted to degradation thereby allowing dl to enter ventral nuclei in the periphery of the embryo (Roth et al., 1989; Steward, 1989; Rushlow et al., 1989). In the nucleus, dl acts as a transcription factor and is required to activate mesoderm (*snail*, *twist*), mesectoderm (*sim*), and neuroectoderm (*rhomboid*, *brinker*, *vnd*, *ind*) differentiation genes in different domains of expression (reviewed by Stathopoulos and Levine, 2005). The nuclear dl distribution displays a concentration gradient that peaks at the ventral midline and decays dorsally, suggesting that dl acts directly as a morphogen gradient (reviewed by Reeves and Stathopoulos, 2009). Moreover, dl has been shown to be *sufficient* to establish different patterns of gene expression in the embryos that have no other source of DV positional information (Huang et al., 1996; Stathopoulos and Levine, 2002). In this study, we use the *Drosophila* embryo as a model to study spatial scaling of DV patterns with respect to natural variations in embryo size. We provide evidence that scaling in this system depends on each particular gene rather than on its location. In addition, we show that the length-scale of the nuclear dl gradient scales with embryo size, but it is not sufficient to explain scaling of dl target genes. We propose that factors downstream of dl contribute to scaling of DV patterns with respect to size in this system.

4.2 Materials and Methods

Fly Stocks

Two "wild-type" populations of embryos were considered. One population comprised embryos of *yw* genotype and the other comprised embryos from the India strain. India embryos are a wild-type strain of *Drosophila melanogaster* that are about 25% larger than the laboratory wild-type strain (*w1118*) along the AP axis (Lott et al., 2007). For the experiments in which the dl gradient is ectopically generated along the AP axis, we collected embryos from females of genotype *wind*[M88]/*wind*[E4]; hsp83>Toll10b bcd 3' UTR. These embryos lacked normal DV patterning due to maternal loss-of-function of the *windbeutel* (*wind*) gene (*wind*[M88] and *wind*[E4] are null alleles; Nilson and Schupbach, 1998). Females carrying the *hsp83*>Toll10b *bcd* 3' UTR (HTB) transgene lay embryos that express an activated form of Toll (Toll10b) maternally-driven by the *hsp83* promoter in the anterior pole of the egg using the *bcd* localization sequence (Huang et al., 1996).

Fixation and Fluorescent *in situ* Hybridization

Two-four hour old embryos were fixed using formaldehyde solution using standard techniques. Fluorescent *in situ* hybridization was performed according to standard protocols using digoxigenin-, biotin- and fluorescin-labelled riboprobes for *sog*, *ind*, and *vnd*. Primary antibodies used were sheep anti-digoxigenin (1:500, Roche), mouse anti-biotin (1:500, Roche) rabbit anti-fluorescin (1:500, Invitrogen), mouse anti-dorsal (1:10, Hybridoma Bank Developmental Studies at the University of Iowa), and rabbit anti-

Histone H3 (1:1000, Abcam). Secondary antibodies used were Alexa Fluor 488 anti-mouse, Alexa Fluor 555 anti-sheep, and Alexa Fluor 647 anti-rabbit (1:1000, Invitrogen).

Embryo Sectioning and Mounting

Fluorescently stained embryos were individually sectioned in 70% glycerol using a sharp razor blade under a dissecting microscope (except for the embryos from *wind*; HTB mothers which were kept as whole-mounts). Sections were taken approximately at 50% egg length and about 150 mm thick (as estimated from comparing with the diameter of the embryo). "Wild-type" sections (and whole embryos from *wind*; HTB mothers) were mounted in 70% glycerol on a glass slide with a cover glass supported by two pieces of double-sided tape in each side to minimize deformation of the sample.

Image Processing, Measurements, and Data Analysis

Statistical analysis was performed using standard tools and functions from MATLAB. Images of fluorescent embryos or sections were taken using a LSM 5 Pascal confocal microscope. Imaging of each sample was performed under identical conditions. To reduce temporal-dependent fluctuations in gene expression, only embryos from late nuclear cycle 14 (marked by expression of *ind*) were considered in the analysis. For "wild-type" cross sections, we acquired an average of 15 z-stacks from the center of the specimen (where deformation of the embryo due to sectioning does not affect the embryo's morphology) using a 40X-oil objective. Z-stacks were then orthogonally projected and gene expression profiles were obtained using MATLAB. Quantification of nuclear dorsal levels in cross sections relative to Histone H3 levels was performed as in a

previous study (Liberman et al., 2009). Measurements of embryo circumference were estimated by calculating the pseudoarclength of 50-100 points found to be on the perimeter of the embryo. In order to obtain the location of the boundaries of the patterns, each gene expression profile was fitted to a stereotypical profile of the specific pattern as described previously (Liberman et al., 2009) and the borders of gene expression were computed as the points of half-maximal decay of the fitted profiles. The location of the ventral midline was found as the average of the midpoints between dorsal and ventral borders of each gene or as the center of the peak of the dorsal gradient.

For whole-mount embryos, we acquired z-stacks from the top of the embryo to about 50% depth using a 20X objective. Each embryo "shell" was then "computationally-unrolled" as described in a previous study (Liberman et al., 2009) to take into account the embryo curvature. The length of the AP axis in each embryo was obtained by computing the average size of the "unrolled" sheet and the positions of the gene expression boundaries were obtained as described above for cross sections. The distance from the anterior pole of the embryo to the locations of target genes was obtained from the "unrolled" sheet and therefore corresponded to distances measured on the surface of the embryo. Quantification of the dl nuclear gradient in whole-mount embryos was obtained by adapting the algorithm of nuclear dl quantification in wild-type embryos published before (Liberman et al., 2009). In embryos from *wind*; HTB females, the nuclear dl gradient is fitted to a Hill function of the form,

$$f(x) = \frac{Ax^m}{k^m + x^m}$$

and the "width" of the gradient is defined as the half-maximal value of the Hill function, "k."

Scaling Criterion

We devised a criterion to determine quantitatively whether or not the location of a certain pattern *scale* with respect to natural variations in the length of the DV axis. For each embryo (labeled by the index i), let X_i be the measured location of a certain pattern with respect to a reference point (in this case, the absolute distance from the border of a certain gene measured to the ventral midline), and let L_i be the length of the embryo's DV axis (estimated by the semi-circumference at approximately mid-embryo along the AP axis). If the population of embryos is sufficiently large, it is possible to study how X_i and L_i are statistically correlated using simple regression analysis. "Perfect scaling" corresponds to the case in which the following linear model holds,

$$X_i = x\, L_i \qquad \text{for all } i, \qquad (4.1)$$

where x is a constant that represents the *relative position* of the pattern. Conversely, if X_i remains unchanged with L_i (i.e., if X_i=x for all i), then X_i and L_i are *not* statistically correlated, and therefore, the location of the pattern is *independent* of embryo size. However, these scenarios are just extreme hypothetical situations and, in practice, there is a continuous range of scaling behaviors in between. A more general and realistic situation is that the pair (X_i, L_i) is linearly correlated while not necessarily obeying the strict scaling condition (4.1), i.e.,

$$X_i = m\, L_i + b \qquad \text{for all } i \qquad (4.2)$$

with m and b some parameters determined by fitting the data to the linear model (4.2). Note that when $|b|$ is "sufficiently" small, the model (4.2) approximates the perfect scaling case (4.1). Note that the model (4.2) also includes the case in which positional

values are independent of size when m=0, which in practice correspond to the case when $b \approx \overline{X}$, where $\overline{X}$ is the mean of the X_i's. However, it is not always possible to make an accurate decision about scalability; for example, if the variability of the positional data (X_i) is "larger" (either due to measurement errors or internal noise) than the range of embryo sizes along the DV axis (L_i) (see below).

We define three steps that provide a simple quantitative criterion to determine scaling in this system:

1. *Scalability Test:* A decision about scalability of the dataset (X_i, L_i) can be made if the range of L_i's is larger than the variation in positional values, X_i's. This is, we say that the dataset (X_i, L_i) *passes* the scalability test if

$$S \equiv \frac{2\,\Delta x\,\overline{L}}{\mathrm{r}(L)} < 1,$$

with Δx the standard deviation of the scaled positions $x_i = \frac{X_i}{L_i}$, $\overline{L}$ is the mean of the L_i's, and r(L) is the "range" of the L_i's as defined by $L_{\max}$ - $L_{\min,}$ where $L_{\max}$, $L_{\min}$ denote the extremes of the distribution of lengths (centered at $\overline{L}$) encompassing 80% of the L_i's. The quantity S will be referred as the *scalability factor*.

2. *Simple linear regression*. A dataset that passes the scalability test is then fitted to a linear model,

$$X = \hat{m}L + \hat{b}, \qquad (4.3)$$

where $\hat{m}$ and $\hat{b}$ are the least-squares estimates of the regression. By construction, the least-squares approximation (4.3) is satisfied by $X = \overline{X}$ and $L = \overline{L}$. Thus, if we write $\hat{b} = \alpha\overline{L}$, then Equation (4.3) evaluated at the mean values takes the following form,

$$\overline{X} = (\hat{m} + \alpha)\overline{L}.$$

Therefore, α is a measure of "how much" the estimated slope would need to be corrected (in units of axis length) in order to have perfect scaling at the point of center of mass ($\overline{X}, \overline{L}$). For practical purposes, we say that a dataset (X_i, L_i) exhibits *strict scaling* if $|\alpha| \leq 0.05$, meaning that linear model of the data differs from the perfect scaling case by at most 5% of the total axis length.

3. *Scaling significance*. Because of the statistical nature of the data, under certain circumstances scaling may be explained by chance, due to random variations in the positional data. This depends on the relative position of the pattern (approximated by $x = \frac{\overline{X}}{\overline{L}}$); confidence about strict scaling increases with the distance from the pattern to the reference point and can be captured in the following quantity,

$$C \equiv \left(1 - S\frac{\overline{L}}{\overline{X}}\right)100\% \qquad \text{if } S\frac{\overline{L}}{\overline{X}} \leq 1 \text{ and } C \equiv 0\% \text{ otherwise.}$$

As the scalability factor S is a measure of the maximum slope that can be generated solely by variability in the positional data, the *scaling percentage, C,* is the percentage of data that *cannot* be explained by the variability in the positional data (see Supporting Fig. 4.1).

4.3 Results

Determining Scaling from Quantitative Measurements of Gene Expression

Using fixed cross sections of wild-type embryos, we quantified the expression levels of three dl target genes that pattern the neuroectoderm of the embryo and measured the positions of their dorsal and ventral borders with respect to the ventral midline along the circumference (Fig. 4.1A,B). We also measured the length of the DV axis as the semi-

circumference of the cross section for each embryo (Fig. 4.1A). In order to study the correlation between pattern locations and size, we devised a criterion to determine scaling of pattern locations with respect to the length of the DV axis in a homogeneous population of embryos (see Materials and Methods for details). Briefly, the criterion determines scalability from three statistical measures. First, the *scalability factor, S*, determines if the range of lengths along the DV axis is larger than the variability of the positional data (scalability test). If the scalability test fails (i.e., if $S>1$) then we cannot conclude anything about the scalability of the pattern location from the data. Second, the *scaling compensation value,* α, measures how positional data compensate to changes in the length of the DV axis based on a linear model of the data. Perfect scaling corresponds to the case in which $\alpha=0$. If $\alpha>0$, then changes in the length of the axis are *undercompensated* by changes in the position of the pattern. Conversely, $\alpha<0$ corresponds to the case in which changes in the length of the axis are *overcompensated* by changes in the position of the pattern. Third, the *scaling percentage, C,* provides a measure of the percentage of data that exhibits scaling beyond what can be explained by chance (i.e., by random fluctuations in our measurements of positional data). This criterion provides a precise definition of scaling from our quantitative gene expression data.

sog and *vnd* Strictly Scale with the Length of the DV Axis, while *ind* Expression Exhibits Overcompensation

Based on our measurements of the position of gene expression patterns with respect to the ventral midline (Fig. 4.1B), we find that the locations of the dorsal borders of *vnd* and *sog* scale almost strictly with the perimeter of the semi-circumference (i.e., the relative

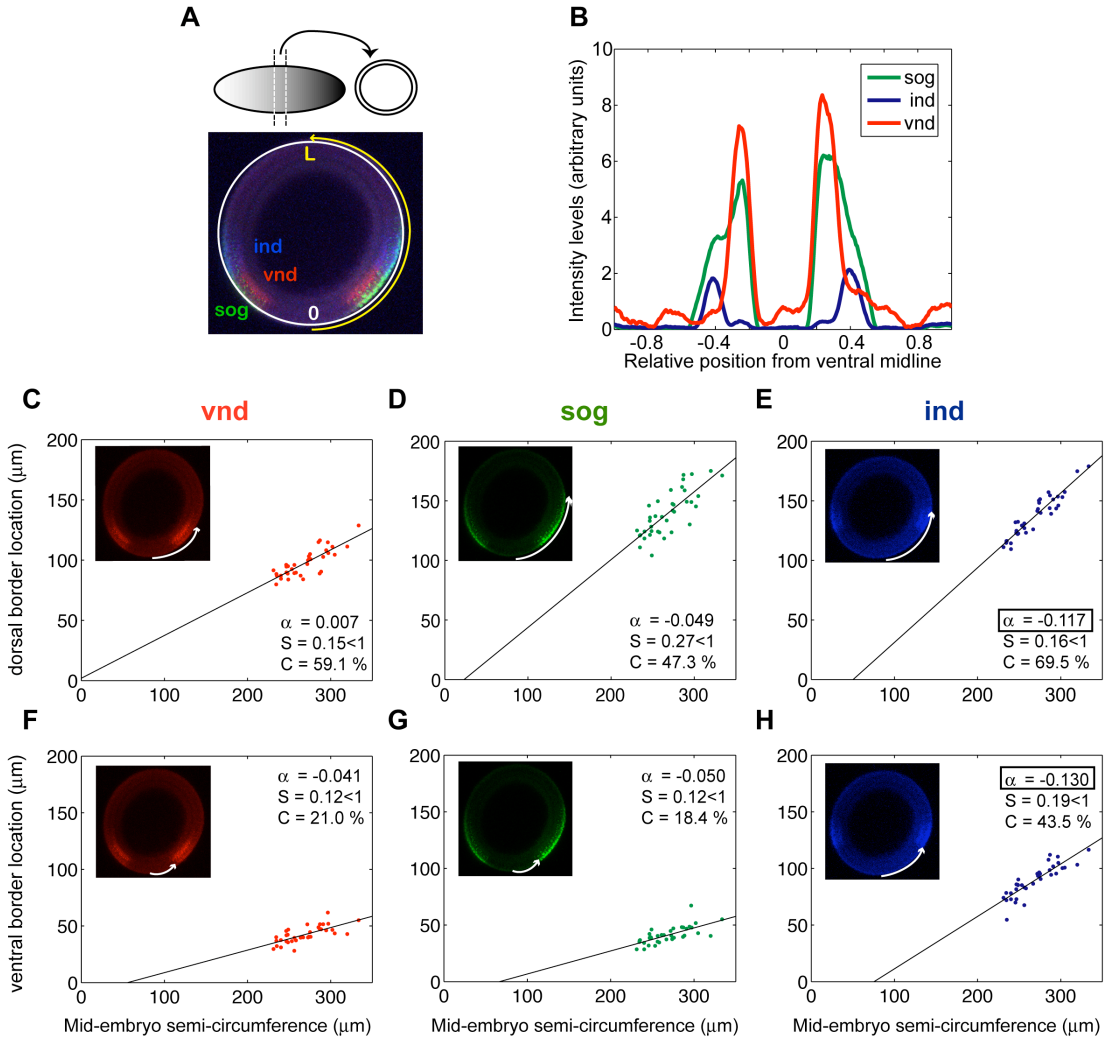

Figure 4.1 Scaling of DV patterns in wild-type embryos.

(A) Fluorescent *in situ* hybridization in a wild-type (*yw*) embryo using *sog* (green), *vnd* (red) and *ind* (blue) probes. Fixed embryos of *yw* phenotype were sectioned approximately at 50% egg length and mounted upright for imaging. The length of the DV axis was measured as half the perimeter of the polygon that encompasses the cross section. Using the ventral midline as a reference point (x = 0), we measured the location of gene expression boundaries around the circumference. **(B)** Gene expression profile around the embryo cross section extracted from the image in (A) in units of DV axis length, L. **(C-H)** Dorsal (C-E) and ventral (F-H) border locations of *vnd* (C,F), *sog* (D,G), and *ind* (E,H), plotted against the length of the DV axis. Each data point displayed corresponds to the average of the distance to each of the two lateral expression domains. Black lines correspond to the least-squares fit of the data. The results of the scaling

criterion applied to each dataset are shown in each panel. By convention, *strict scaling* occurs if $S<1$ and $0.050 \leq \alpha \leq 0.050$.

---

positions are within 5% ($|\alpha| < 0.05$) of the expected (strict scaling) locations with ~50% or more of scaling percentage; Fig. 4.1C,D). Similarly, the locations of the ventral borders of *vnd* and *sog* appear to strictly scale with size, although the scaling percentages of these data are somehow lower (~20%; Fig. 4.1F,G). Collectively, these data provide evidence that the ratios of the "width" of the *vnd* and *sog* patterns to the length of the DV axis remain constant. The positions of the *ind* borders also correlate with changes in the size of the embryo, but this correlation exhibits overcompensation, i.e., variations in the length of the axis result in larger "shifts" of the borders' locations compared to those expected by strict scaling (Fig. 4.1E,H). Therefore, the extent to which scaling is attained depends on the genetic identity of each pattern rather than on its position within the axis (see Discussion).

The dl Gradient also Scales with Respect to the Length of the Embryo Circumference, but it is Insufficient to Explain Scaling of its Target Genes

Since dl controls patterning of the DV axis, we examined whether scaling of *sog* and *vnd* was a direct consequence of scaling of the dl gradient. The dl gradient has a bell-shaped profile that can be empirically fitted to a Gaussian distribution of the form

$$dl(x) = A\exp\left[-\frac{x^2}{2\sigma^2}\right] + B, \qquad (4.4)$$

with A denoting the amplitude of the gradient and σ denoting its "width" or decay length (Liberman et al., 2009; Fig. 4.2A,B). As a consequence of the dl-gradient shape, any two gradients of widths σ and $(1+\gamma)\sigma$ (with γ a small perturbation) are shifted from one

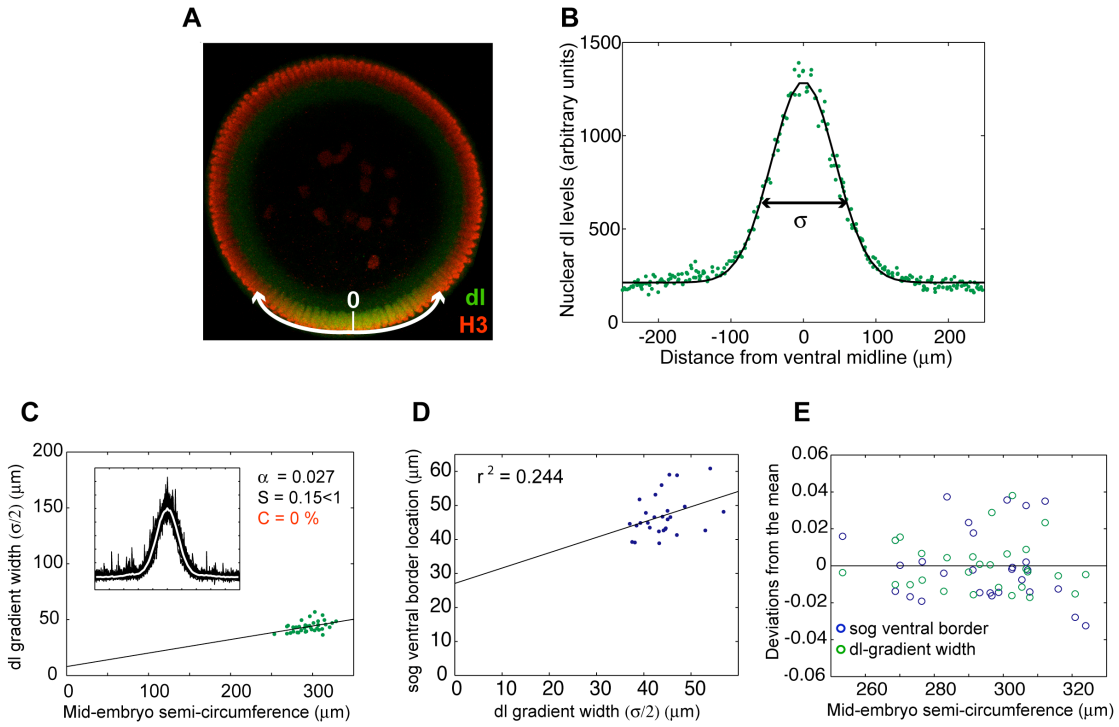

Figure 4.2 Scaling of the nuclear dl gradient in wild-type embryos.

(A) Immunostaining of a wild-type (*yw*) cross section taken at mid-embryo using dl (green) and Histone H3 (red) antibodies to quantify nuclear dl intensity levels. **(B)** Quantification of nuclear dl levels around the cross section circumference using the ventral midline as a reference point (x = 0). Each (green) data point corresponds to the average dl intensity in each nucleus detected by the segmentation algorithm displayed according to its distance from the reference point (x = 0). Black curve indicates the best fit of a Gaussian function of the form of Equation (4.4) characterized by the decay-length, σ. **(C)** "Widths" of the nuclear dl gradient defined as half of the decay-length (σ/2) of the fitted Gaussian curve plotted against the length of the DV axis. Inset shows the intensity profiles of all the embryos considered (n=38). **(D)** Position of the ventral border of *sog* compared to the width of the nuclear dl gradient in the same embryos. The black line represents the least-squares fit to the data points (and *r* denotes the correlation coefficient). **(E)** Precision in the width of the dl gradient vs. precision in determining the ventral boundary of *sog*. Each data point in the graph corresponds to the difference between scaled position (X_i / L_i) of the ventral border of *sog* in an embryo and the mean relative location (or the difference between scaled widths (σ_i / L_i) in an embryo and the mean scaled width) as a function of the mid-embryo semi-circumferences (L_i).

another by exactly the same proportion (1+γ) at any concentration threshold. For example, two gradients whose widths differ by 10% will differ by exactly 10% at the concentrations required to define different patterns of gene expression. Therefore, it is reasonable to use the width of the gradient, σ, as an indicator of how the dl gradient is affected by variations in the length of the DV circumference. We quantified the nuclear levels of dl in fixed cross sections of wild-type embryos and found that the width of the gradient scales with the size of the axis (Fig. 4.2C). However, we found that these data have a scaling percentage of C=0%, i.e., it is not possible to rule out that scaling of these data can be fully explained by the internal variability or experimental error in the measurements of the dl widths. A way to increase the scaling percentage C is to consider a broader range of DV axis lengths. We attempted to increase r(L), by considering the wild-type strain India, whose embryos are ~25 % larger along the AP axis compared to the laboratory strain (Lott et al., 2007). However, we did not find any significant difference in length along the DV axis (see Supporting Fig. 4.2). Nonetheless, we asked if the presumptive scaling of the dl-gradient width could explain scaling of the target gene expression patterns. We stained wild-type embryos simultaneously with dl/Histone H3 antibodies and *sog* RNA probe and asked whether or not the width of the dl gradient correlates with the ventral position of *sog*. Our data show that the location of the ventral border of *sog* is slightly correlated with the width of the dl gradient (r^2=0.244; Fig. 4.2D). However, this correlation is not sufficient to explain scaling of this pattern with respect to the length of the DV axis because changes in dl gradient widths are under-compensated by changes in the location of the *sog* expression pattern (Fig. 4.2D).

These data also provide the opportunity to compare the precision of the dl gradient with the precision in determining the ventral location of the *sog* pattern. We found that the precision in defining the location of the ventral border of *sog* is similar to the precision of the width of the gradient (Fig. 4.2E). This observation demonstrates that the dl gradient could be able to determine the relative location of the ventral border of *sog* with the observed precision. Therefore, the positional information encoded by dl is insufficient to determine the relative position of the *sog* pattern in a concentration-dependent manner.

Taken together, our results reveal that the width of the dl gradient scales with respect to the DV circumference, but scaling of the ventral border of *sog* cannot be explained by a proportional shift of the dl gradient, and suggest that other factors participate in establishing the relative location of this pattern. For example, it is possible that dl contributes to setting the location of the borders of gene expression factors, but additional factors are required to "sharpen" this location as a function of the length of the DV axis.

Scaling of DV Patterns Depends on Factors Downstream of the Toll Pathway

Our data suggest that additional factors are required to determine the relative location of gene expression patterns. Previous models suggest that scaling might be explained by a combination of gradients emanating from opposite ends of a single axis (Aegerter-Wilmsen et al., 2005; Hörstadius, 1939; McHale et al., 2006; Wolpert, 1969). In order to test whether a gradient established from the dorsal side of the embryo contributes to scaling of dl target genes, we use a genetic background in which DV patterning is

ectopically established along the AP axis. Embryos from females that are mutants for at least one of the factors that disrupt DV patterning [such as *windbeutel* (*wind*)] and in addition, carry the HTB transgene (a maternal promoter Hsp83 used to express an activated form of the Toll receptor (Toll10b) using the *bcd* localization sequence), exhibit a full range of DV patterns along the AP axis (Huang et al., 1996). While ectopic DV patterns along the AP axis in embryos of this genetic background cannot be directly compared to endogenous patterning along the DV axis of wild-type embryos, this system allowed us to investigate whether or not endogenous factors are required for scaling of dl-target genes. Since activated Toll is the only source of ectopic DV positional information in these embryos, we would expect that the dl-target genes will lose their ability to scale with respect to the length of the axis if scaling were dependent on additional endogenous factors (e.g., an opposing gradient emanating from dorsal regions of the embryo). We quantified the gradient of nuclear dl in whole-mount embryos from *wind*; HTB mothers and observed several differences with respect of the endogenous dl gradient (Fig. 4.3A-C). First, the overall shape of the gradient is "bimodal" instead of Gaussian (Fig. 4.3B). Second, we observed a very high embryo-to-embryo variability in the range of the dl nuclear gradient. Figure 4.3B shows representative nuclear dl gradients from three different embryos in which such variability is clearly exhibited. Third, unlike in the wild-type case, the width of the ectopic dl gradient does not correlate with the length of the AP axis (Fig. 4.3C).

Next, we measured the distance from the anterior pole of the embryo to the "posterior" borders of *vnd*, *sog*, and *ind* (Fig. 4.3D), i.e., those that would correspond to the dorsal borders in wild-type embryos. Strikingly, the location of the *vnd* border strictly

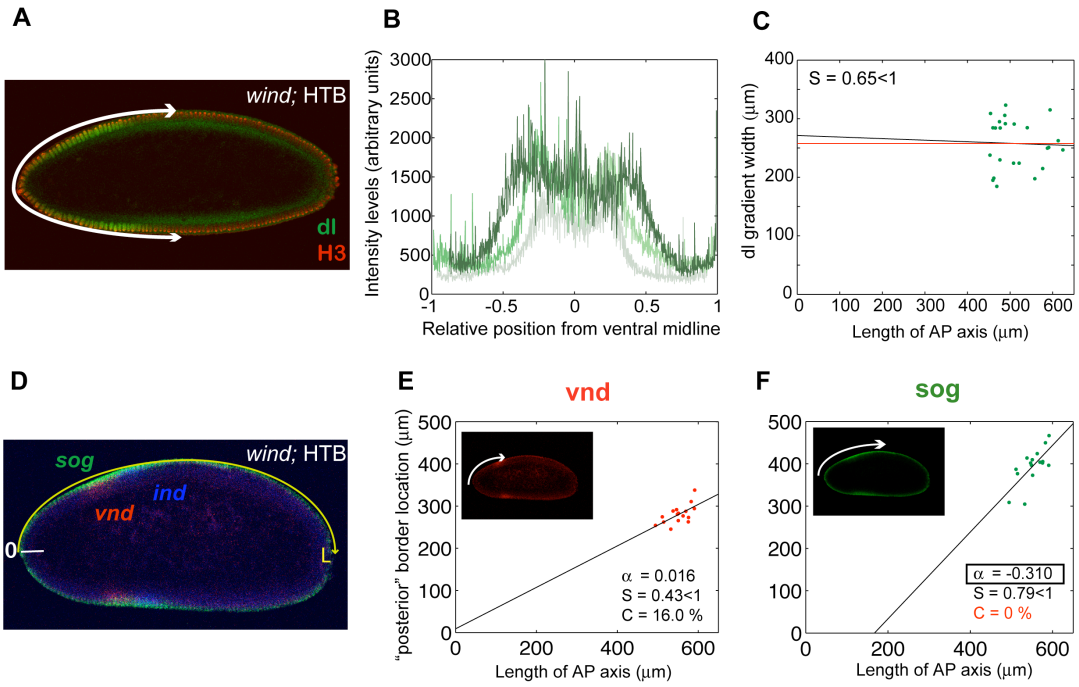

Figure 4.3 Scaling of dl and dl-target genes along the AP axis in embryos from *wind*; HTB females

(A) Immunostaining of an embryo from a *wind*; HTB female using dl (green) and Histone H3 (red) antibodies to quantify nuclear dl intensity levels. **(B)** Intensity profiles from three different embryos that illustrate the variability in the width of the nuclear dl gradient in this genetic background. **(C)** In contrast to the wild-type case, the nuclear dl gradients in this genetic background are fitted to the shape of a Hill function and the "width" is defined as the fitted parameter *k* in the Hill equation (see Materials and Methods). The width of the nuclear dl gradient in these embryos is plotted against the length of the AP axis along the surface of the embryo. The least-squares fit of the data (black line) is similar to a horizontal line that defines the mean width (red line). **(D)** Fluorescent *in situ* hybridization in an embryo from a *wind*; HTB female using *sog* (green), *vnd* (red) and *ind* (blue) probes. The location of borders of gene expression and the length of the AP axis were measured on the surface of the embryo using the anterior pole as a reference point (x = 0). **(E, F)** The position of the posterior borders of *vnd* (E) and *sog* (F) are plotted against the length of the AP axis. Black lines correspond to the least-squares fit of the data. The numerical results of the scaling criterion applied to each dataset are shown in each panel.

scales with the length of the AP axis (Fig. 4.3E). Although the level of scaling percentage in this case is significantly lower than in the wild-type case, this result is remarkable considering that the scalability of the dl gradient widths is completely abolished in this system (Fig. 4.3C). In contrast, the borders of *sog* and *ind* do not seem to scale along the AP axis and exhibit a high degree of embryo-to-embryo variability (Fig. 4.3F and data not shown). The result that *vnd* scales in this system suggests that the mechanism for "sensing" the size of the embryo to establish relative positional information must depend on factors downstream of Toll signaling activation.

4.4 Discussion

A balanced relationship between pattern and size in embryonic development is essential to produce well-proportioned organisms. Although this relationship has been extensively studied in embryological systems such as frogs and sea urchins by dissection and transplantation experiments (reviewed by De Robertis, 2006), little is known about the interplay between pattern and size in natural populations. In this work, we investigated the correlation between patterns of gene expression and embryonic length along the DV axis in the *Drosophila* embryo. In summary, our results provide evidence that the dl-target genes *vnd* and *sog*, as well as the dl gradient itself, exhibit scaling over a range of embryo sizes. However, our data show that scaling of the dl gradient is neither necessary nor sufficient to explain scaling of gene expression patterns along the DV axis. We propose that gene-specific feedback mechanisms operate downstream of the dl gradient to provide positional information relative to the size of the system.

Spatial Scaling of DV Patterns is a Gene-Dependent rather than a Position-Dependent Property

Our data provide evidence that while the ventral boundaries of *sog* and *vnd* coincide (Fig. 4.1B) and scale with respect to the DV circumference (Fig. 4.1F,G), under certain conditions (e.g., in embryos from *wind*; HTB females) scaling of one border does not imply scaling of the other. Similarly, the dorsal border of *vnd* often coincides with the ventral border of *ind*, but our data show that these boundaries have different scaling behaviors (Fig. 4.1C,H). These results support the idea that scaling in this system depends on the gene in question rather than on its location.

Interestingly, this conclusion is in contrast with a recent study on scaling of gap genes along the AP axis of the *Drosophila* embryo that suggest that scaling in the posterior half of the embryo occurs regardless of the gene assayed (de Lachapelle and Bergmann, 2010). Another intriguing difference between our findings on DV patterning and recent work on scaling along the AP axis is the role of the participating morphogens. In the case of Bcd, there is recent evidence that its distribution scales precisely along the AP axis and correlates with the positions of target gene expression (Gregor et al., 2007; He et al., 2008; He et al., 2010). In contrast, while our data suggest that the nuclear dl gradient might scale with the embryo circumference, scaling of the gradient does not necessarily imply scaling of target genes (Fig. 4.2C,D).

Mechanisms of Spatial Scaling along the DV Axis

While the role of dl as the main player in DV patterning in the *Drosophila* embryo cannot be questioned, our results challenge the idea that a gradient of dl provides directly enough positional information to explain scaling of the DV patterns assayed. In particular, our

observations that scalability of the dl gradient does not imply scalability of gene expression patterns leave doubts regarding the mechanisms of establishing relative positional information in this system.

Although our data do not reveal the mechanisms underlying scaling in this system, it does restrict the set of possible scenarios. For example, our observation that the ventral border of *vnd* scales in embryos from *wind*; HTB mothers suggest that the mechanism of scaling of this border should depend on factors that are downstream of Toll signaling. In particular, our data rule out the possibility that two independent gradients emanating from opposing regions establish relative coordinates of positional information in the system (Wolpert, 1969). However, we cannot discard the possibility that two "interdependent" gradients are involved –for instance, an opposing gradient that depends on dl may be required for scaling. One attractive candidate for this opposing gradient is *decapentaplegic* (*dpp*), a member of the TGF-β family. *dpp* expression is restricted to the dorsal-most part of the embryo by dl, and key regulators of Dpp signaling such as *sog* and *brinker* are also under direct transcriptional control by dl (François et al., 1994; Jazwinska et al., 1999). These facts suggest that *dpp* could take part in a feedback mechanism that contributes to establishing a scale-free coordinate system along the DV axis. However, our preliminary results do not show defects on *vnd* scaling in *brk*, *sog* double mutant embryos (data not shown).

Origin of Relative Positional Information in DV Patterning

The elegance of the Classical Morphogen model relies on providing patterning information from a single input: the concentration distribution of the morphogen. As a

consequence, a gradient that scales with size results in patterns of gene expression that scale accordingly. In contrast to this view, our data suggest that positional information relative to the length of the DV axis cannot be established from the simple readout of the dl nuclear gradient (Fig. 4.4A). Instead, our results suggest that the dl gradient can only *instruct* directly a region that is subsequently "sharpened" to a precise location by downstream mechanisms that are specific to each gene (Fig. 4.4B). For example, scaling of the border of *sog* should depend on scaling of the dl-gradient because *sog* scaling is disrupted in embryos from *wind*; HTB mothers (Fig. 4.3F). However, the dl-gradient is insufficient to determine the relative position of *sog* boundaries (at least linearly in a concentration-dependent manner), as the *sog* ventral border does not compensate as much as it would be predicted by a direct readout of the nuclear dl gradient (Fig. 4.2D). Perhaps, scaling of the dl-gradient ensures scaling of other factors (e.g., repressors of *sog* expression) that directly result in scaling of *sog* borders along the DV circumference (Fig. 4.4B). The case of *vnd* is even more dramatic as it does not appear to require scaling of the dl gradient (Fig. 4.3E) suggesting that downstream factors can self-organize scaling of the ventral border of *vnd* with respect to axis length. Some obvious candidates to fulfill the role of these downstream factors that are already known to participate in "sharpening" the ventral borders of *vnd* and *sog* are the transcription factors Twist and Snail (von Ohlen and Doe, 2000; Cowden and Levine, 2003). Future work will determine whether or not Twist and Snail are required for determining the location of the ventral borders of *sog* and *snail* in coordinates relative to the length of the axis.

While the cases examined here do not appear to rely on scaling of the dl gradient to ensure scaling of target gene expression, we cannot rule out that other dl target genes

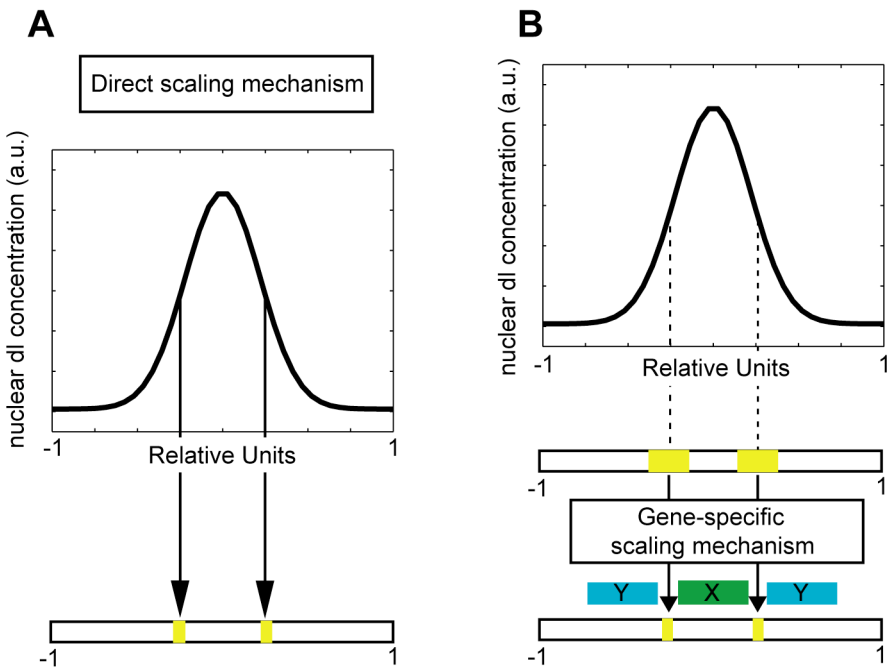

Figure 4.4 Models of spatial scaling of DV patterns in *Drosophila.*

(A) In the *direct scaling mechanism*, a scaled dl gradient defines scaled locations of gene expression. The mechanism of scaling in this case is probably upstream of dl (e.g., scaling of the *pipe* domain in ovarian egg chambers). Although it is possible that some dl-target genes scale as a consequence of nuclear dl scaling, none of the genes assayed here correspond to this case. **(B)** Scaling of the DV patterns studied here is gene-specific. Even if the dl gradient scales with the length of the DV axis, additional downstream factors X and Y could be required for scaling of other dl-target genes. These factors are likely gene-specific, rather than position-specific.

---

scale as a direct consequence of scaling of the dl gradient (Fig. 4.4A). Therefore, an important question is how a scale-invariant dl gradient is established in the first place. One possibility is that feedback mechanisms exist that ensure that the dl gradient accommodate to the size of the embryo (see Ben-Zvi and Barkai (2010), for example). Our data however, do not support the idea that feedback interactions downstream of dl control scaling of the nuclear dl gradient itself because the gradient fails to scale in

embryos from *wind*; HTB females. Another possibility that is consistent with previous studies is that scaling of the dl gradient results from scaling of an upstream factor in the DV signaling cascade. In ovarian egg chambers, *pipe* is expressed in the 40% ventral most region of the follicular epithelium around the oocyte irrespective of egg size (Nilson and Schupbach, 1998; Peri et al., 2002). Since *pipe* predefines the location of the nuclear dl gradient in the embryo, these studies suggest that scaling of the dl gradient may result from scaling of the *pipe* expression domain in the oocyte. Thus, it is conceivable that an ancestral mechanism of scaling that originates in the oocyte and results in scaling of the dl gradient and other dl-dependent patterns diverged at some time in evolution in order to provide more complex mechanisms that ensure the proper establishment of relative positional information in a gene-specific manner.